


X-ray diffraction as a major tool for the analysis of PM_{2.5} and PM₁₀ aerosolsNasser M. Hamdan ^{1,2,a)} and Hussain Alawadhi²¹Physics Department, American University of Sharjah, Sharjah, United Arab Emirates²Center for Advanced Materials Research, University of Sharjah, Sharjah, United Arab Emirates

(Received 11 March 2020; accepted 16 March 2020)

Particulate matter (PM) specimens from a traffic site were sampled on Teflon filters using a low volume sampler. The sampling campaign ran over a one-year period with sampling frequency of twice a week for both PM_{2.5} and PM₁₀. X-ray diffraction (XRD) methods, which are not commonly used in PM analysis, have been utilized successfully to identify crystalline phases present, including secondary pollutants. XRD data confirmed results obtained by X-ray fluorescence, positive matrix factorization modeling, and scanning electron microscopy. PM_{2.5} consisted mainly of secondary sulfates, like Mascagnite [(NH₄)₂SO₄], Koktaite [(NH₄)₂Ca(SO₄)₂ · H₂O], and Gypsum [CaSO₄ · 2H₂O]. For PM₁₀, it was found that the major phases are mostly originating from natural sources, such as dust storms and sea salts, in addition to secondary compounds, such as sodium nitrate. The main phases identified were Calcite, Quartz, Gypsum, Halite, and Palygorskite. © The Author(s), 2020. Published by Cambridge University Press on behalf of International Centre for Diffraction Data. [doi:10.1017/S0885715620000184]

Key words: particulate matter (PM) specimens, positive matrix factorization (PMF)

I. INTRODUCTION

Particulate matter (PM) pollution is of great concern because of its adverse health and environmental impacts (Widziewicz *et al.*, 2016; Wong *et al.*, 2016). Ambient air pollution is believed to be a major environmental risk for disease and premature death in the United Arab Emirates (Bener *et al.*, 2009; Li *et al.*, 2010; Anderson *et al.*, 2012; Hamdan *et al.*, 2015, 2016, 2018a, 2018b). The UAE is located in an arid region with less than 50 mm average annual rain, large expanses of deserts, and frequent dust storms (NCMS, 2019). These factors adversely affect the precipitation of the suspended dust, particularly its fine fraction. In addition to natural pollutants, anthropogenic sources due to the rapid development of the country through mega oil and construction projects have contributed greatly to the fine PM pollution (Al Katheeri *et al.*, 2012). Traffic is also a major source of fine and heavy element pollutants (Young *et al.*, 2012; Sundvor *et al.*, 2013). Identification of pollution sources is a major task and responsibility for the scientists in order to identify these sources and suggest mitigation solutions.

X-ray fluorescence (XRF) and elemental analysis are commonly used in the study of aerosol pollution, supported by modeling and statistical analysis to identify possible sources of groups of elements [see, e.g., Moloi *et al.* (2002)]. Although it is a very useful approach, it is short of identifying chemical structures (or compounds) of various pollutants. X-ray diffraction (XRD) can identify various crystallographic phases present in the PM and help in finding various sources, particularly the secondary pollutants that are formed in the atmosphere.

In this work, we have sampled PM₁₀ (which stands for PM with an average aerodynamic diameter of less than 10 μm) and PM_{2.5} (with an average aerodynamic diameter of less than 2.50 μm). PM was sampled on Teflon filters following standard sampling protocols. Fine particles (PM_{2.5}) are potentially of greater concern than PM₁₀ for human health because they can penetrate deeply into the lungs, causing extensive damage. They can even get into the bloodstream, increasing the risk of cancer and respiratory, cardiovascular, and ischemic heart diseases. The filters were subjected to gravimetric analysis, XRF (for elemental quantification), black carbon content analysis, XRD, and positive matrix factorization (PMF) modeling (Achilleos *et al.*, 2016). In this paper, only XRD results will be presented and discussed in conjunction with some supporting SEM/EDS images, XRF elemental results, and PMF results.

II. EXPERIMENTAL

The collection site was chosen to correspond to traffic pollution sources. The site is near a major highway in Sharjah (the United Arab Emirates) with coordinates 25°20′39.2″N and 55°26′46.4″E, as shown in Figure 1. We have used the air quality monitoring station for Bee'ah, an environmental management company in Sharjah. It is located about 100 m from the center of a highway. The highway is usually congested from 7:00 am to 10:00 am and in the afternoon from 4:30 pm to 8:30 pm. Sampling was performed using two Sven Leckel LVS/LVS6-RV low volume sampling stations located side by side for both PM₁₀ and PM_{2.5}. PM samples were collected for 24 h twice a week (every Tuesday and Friday) using the European standard (EN12341 2.3 m³ h⁻¹).

XRD measurements were done using a Bruker D8 ADVANCE system equipped with a Cu tube and a linear detector (LYNXEYE XE). The excitation voltage used was 40 kV with a current of 40 mA. The scans were done in the

^{a)} Author to whom correspondence should be addressed. Electronic mail: nhamdan@aus.edu





Figure 1. (Color online) (a) Sampling site near Sharjah International airport highway with coordinates 25°20'39.2"N and 55°26'46.4"E and (b) sampling stations.

2θ range of 5–55° with 0.02° step size and a collection time of 5 s per point. After background removal, the different phases were identified using the ICDD database PDF-4+ Release 2019 (Gates-Rector and Blanton, 2019).

XRF measurements were performed on a Thermo Scientific ARL Qunt'X XRF system under vacuum, with an exposure time of 300 s. Elemental concentrations were calculated in $\mu\text{g m}^{-3}$, using a calibration procedure that involved Micromatter standard thin films and the NIST aerosol Standard Reference Material 2783. SEM/EDS images and elemental maps were performed on a TESCAN environmental scanning electron microscope (VEGA3 XMU). The electron beam excitation was 20 kV, and low vacuum (10 Pa) was used to avoid charging effects on the filters.

EPA PMF Version 5.0 (released 2014) was used to perform the source apportionment studies on both $\text{PM}_{2.5}$ and PM_{10} samples. The PMF modeling quantifies the contribution of sources to samples based on the composition and fingerprint of different sources.

III. RESULTS AND DISCUSSION

A. $\text{PM}_{2.5}$

Figure 2 shows representative XRD patterns for two $\text{PM}_{2.5}$ filters. Sample No. 60 was collected on July 13, 2018, while sample No. 80 was collected on October 5, 2018. The mass concentrations of $\text{PM}_{2.5}$ on these two days were 72 and 77 $\mu\text{g m}^{-3}$, respectively, much higher than the international standards and the average mass concentrations for the whole year. The main two phases present are Mascagnite $[(\text{NH}_4)_2\text{SO}_4]$ and Koktaite $[(\text{NH}_4)_2\text{Ca}(\text{SO}_4)_2 \cdot \text{H}_2\text{O}]$. The peaks of Mascagnite are marked with M, while those of Koktaite are marked with K. Peaks marked with T are coming from the Teflon filters. Sample No. 60 has traces of Chlorite–serpentine $[(\text{Mg,Fe})_6\text{AlSi}_3\text{O}_{10}(\text{OH})_8]$ marked as Ch, a mineral phase consisting of magnesium and iron silicates that have a similar layered crystal structure as Chlorite.

Mascagnite and Koktaite are the dominant phases in $\text{PM}_{2.5}$. Mascagnite is a secondary pollutant formed by the conversion of sulfur dioxide $[\text{SO}_2]$ gas generated from traffic, power plants, and various industries because of fossil fuel burning into fine particles. With the high temperatures, abundance of sunshine, and high relative humidity in Sharjah, oxidation of the SO_2

gas phase by hydroxyl radical (OH) produces sulfuric acid (H_2SO_4), which then interacts with ammonia (NH_3) to form the ammonium sulfate's fine particles ($<0.5 \mu\text{m}$ in diameter) (Ianniello *et al.*, 2011). Calcite $[\text{CaCO}_3]$ that is present in the atmosphere reacts with the ammonium sulfate, at a rate measured in days, to yield Koktaite as an intermediate product and, finally, Gypsum $[\text{CaSO}_4 \cdot 2\text{H}_2\text{O}]$. Gypsum appears mostly in PM_{10} (Satsangi and Yadav, 2014; Song *et al.*, 2015).

Other mineral phases such as Quartz $[\text{SiO}_2]$, Calcite and salts such as Halite $[\text{NaCl}]$ and sodium nitrate $[\text{NaNO}_3]$ have been observed by SEM/EDS elemental maps and by XRF but are not seen by the XRD method in $\text{PM}_{2.5}$ samples. This is because XRD is a bulk technique that is not suited to identifying low concentration phases. Figure 3 shows the SEM image and elemental maps for part of sample No. 58, sampled on July 6, 2018. The maps clearly show NaCl crystals scattered on the image.

XRF results revealed the concentration of various elements and their uncertainties that were used as input to PMF, together with PM mass and black carbon contents, revealing seven sources of pollutants, as shown in Figure 4. Quantitative analysis of elemental compositions obtained by XRF showed that the sulfur content in $\text{PM}_{2.5}$ was the highest among all other elements with an average value over the whole year of $(4.95 \pm 0.55) \mu\text{g m}^{-3}$. This is consistent with the output of the PMF calculations that revealed 42% of $\text{PM}_{2.5}$ sources are sulfates.

Similar results are shown for samples collected on very clear days with $\text{PM}_{2.5}$ mass concentrations equal to or much less than the WHO standard of 25 $\mu\text{g m}^{-3}$. This is shown in Figure 5 for samples 14 and 24 collected on January 14 and March 2, 2018 with $\text{PM}_{2.5}$ mass concentrations of 25 and 19 $\mu\text{g m}^{-3}$, respectively.

B. PM_{10}

Figure 6 shows the XRD pattern for PM_{10} specimens No. 8 and 12, sampled on February 20 and March 6, 2018, respectively. The patterns show the presence of several primary pollutants, such as Palygorskite $[(\text{Mg, Al})_2\text{Si}_4\text{O}_{10}(\text{OH}) \cdot 4(\text{H}_2\text{O})]$, Chlorite–serpentine $[(\text{Mg,Fe})_6\text{AlSi}_3\text{O}_{10}(\text{OH})_8]$, Quartz, Calcite, and Gypsum, and salts such as Halite and sodium nitrate. Mascagnite and Koktaite, two secondary phases that were present in the fine fraction ($\text{PM}_{2.5}$), are also observed by XRD and EDS elemental maps. The primary pollutants are originating from natural sources such as dust storms,

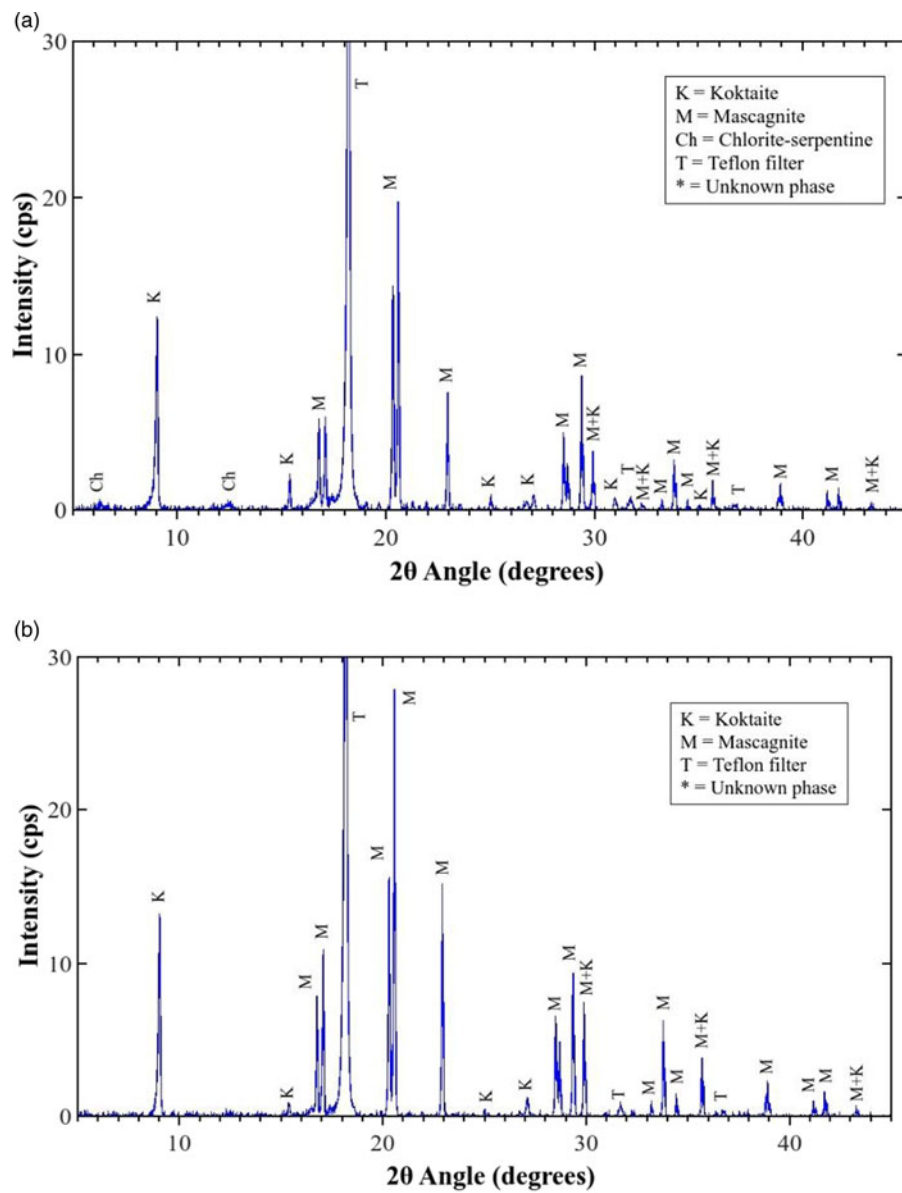


Figure 2. (Color online) XRD patterns of samples PM_{2.5} No. (a) 60 and (b) 80, showing two major secondary pollutant phases, in addition to peaks coming from the Teflon filter.

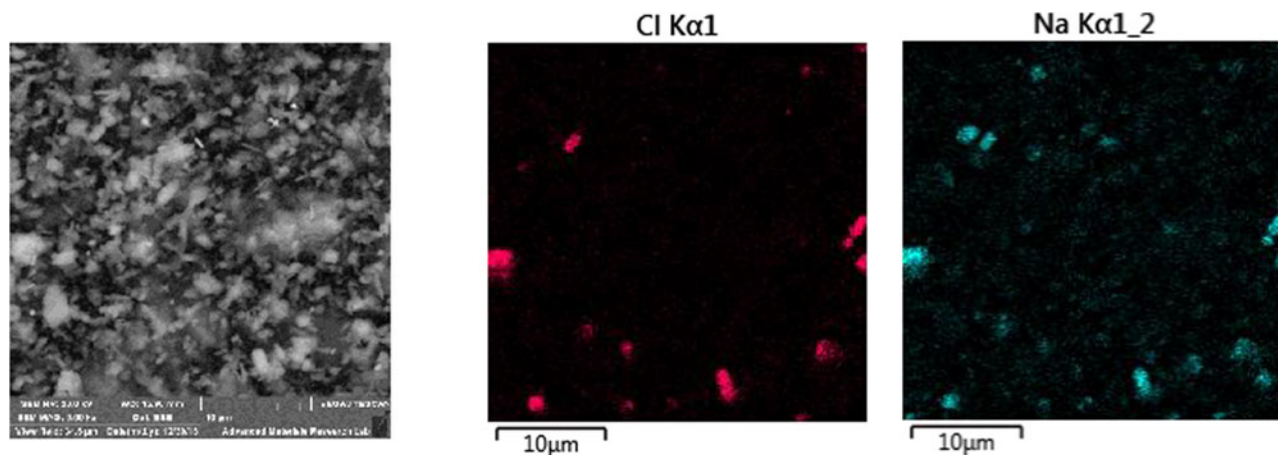


Figure 3. (Color online) SEM and EDS elemental maps of Na and Cl showing good correlation for small NaCl crystals $\sim 1 \mu\text{m}$.

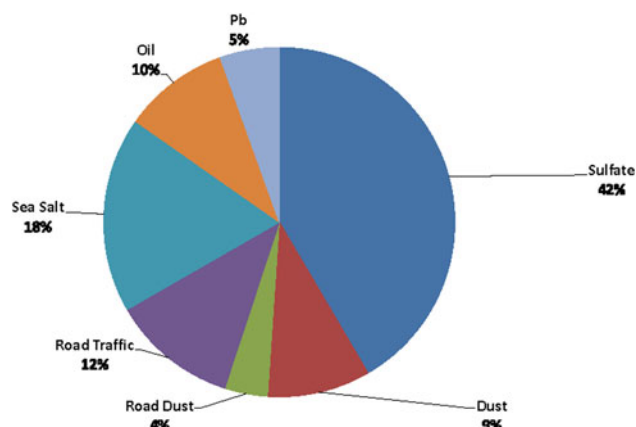


Figure 4. (Color online) PMF result showing seven different sources of pollution. Lead (Pb) is originating from a nearby car-battery recycling plant.

crustal and building materials, and sea salts. The elements of these compounds were all observed in the XRF analysis. Quartz, for example, is a major constituent of desert dust in the UAE, a phase that was clearly observed in the XRD patterns of all PM₁₀ samples. This result is consistent with the quantitative elemental analysis by XRF, in which the average Si content of PM₁₀ over the whole sampling period was found to be $(15.0 \pm 1.5) \mu\text{g m}^{-3}$. Calcite, a crustal and building material, was also observed in the XRD patterns of all PM₁₀ samples, which was identified by XRF as a major pollutant with an average Ca content of $(18.2 \pm 2.4) \mu\text{g m}^{-3}$. In contrast, the average sulfur content in PM_{2.5} and PM₁₀ samples were similar $(5.2 \pm 0.6 \mu\text{g m}^{-3})$, indicating that most of the sulfur is present in the fine fraction of PM₁₀. Although Gypsum, which was observed in PM₁₀, could be of crustal origin, it is believed that it is mostly a secondary phase formed by the interaction of Koktaite with Calcite particles, as mentioned earlier. This is evident from the similarity of the average sulfur content obtained by XRF for both PM₁₀ and PM_{2.5}. Both PM

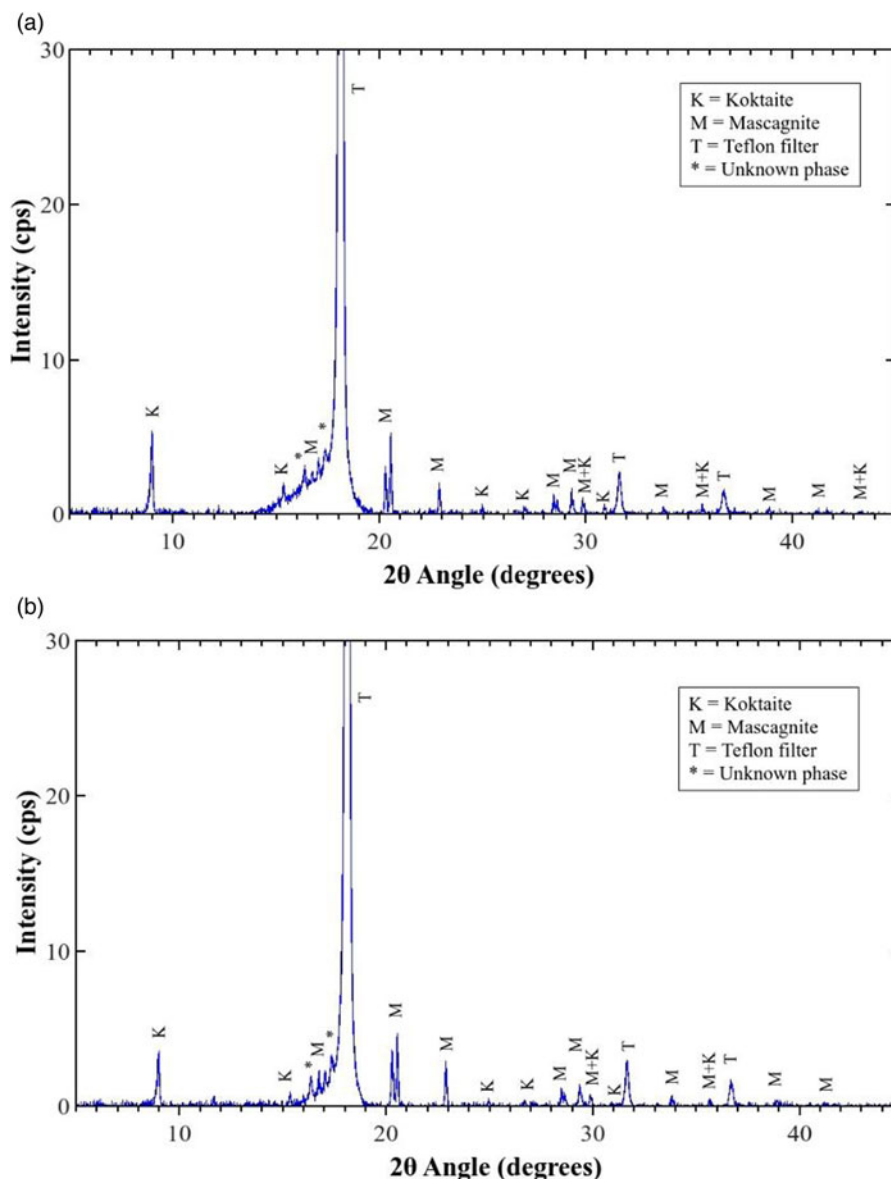


Figure 5. (Color online) XRD patterns of PM_{2.5} samples No. (a) 14 and (b) 24, showing two major secondary pollutant phases, in addition to peaks coming from the Teflon filter.

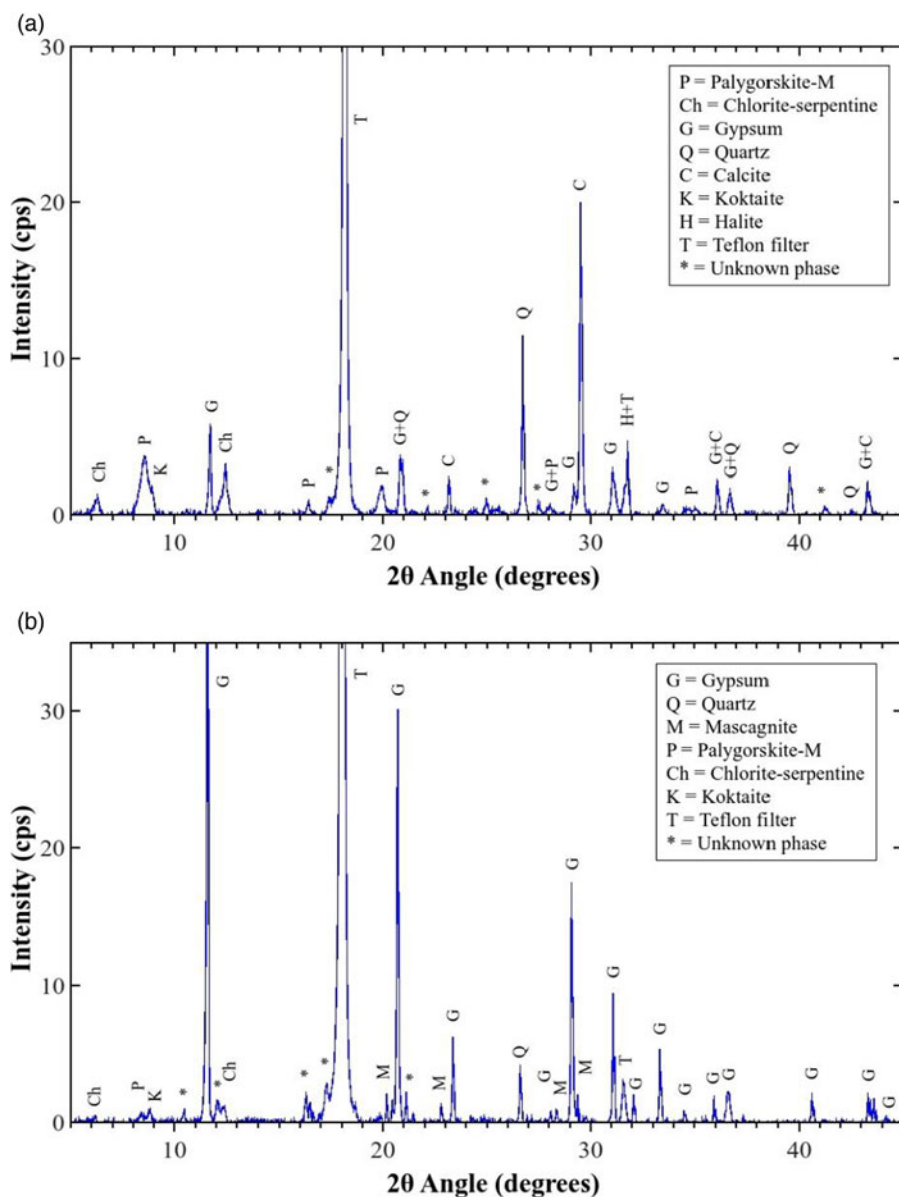


Figure 6. (Color online) XRD patterns of PM₁₀ samples No. (a) 8 and (b) 12, showing the presence of several mineral phases, in addition to Mascagnite and Koktaite.

sizes were sampled simultaneously at the same site using identical sampling stations and protocols, suggesting that the equal sulfur contents observed in PM_{2.5} and PM₁₀ are only due to those in PM_{2.5}, which is coming from secondary sources.

IV. CONCLUSIONS

XRD measurements were used to identify the chemical phases present in the atmosphere by analyzing both fine and coarse aerosol samples: PM_{2.5} and PM₁₀. In addition to the commonly used XRF technique that identifies the elemental composition of pollutants, XRD can be used to determine the major phases present in these pollutants. It was found that the fine PM fraction (PM_{2.5}) contains two dominant secondary phases, Mascagnite and Koktaite, that form by the interaction of gaseous emissions and dust particles in the atmosphere. Black carbon is another main constituent of the fine fraction, which is not detectable by X-ray techniques. In contrast, PM₁₀ was found to include several primary

pollutants such as crustal minerals and sea salts. It also contained Mascagnite and Koktaite that originate from the fine fraction of PM₁₀. XRD measurements were used to identify the chemical states of several elements that constitute atmospheric aerosols such as sulfur, silicon, calcium, sodium, magnesium, and chlorine. The technique has enabled us to identify natural primary and secondary pollutants, which will help in identifying the sources. The XRD results are consistent with the results obtained by XRF and the PMF modeling, as indicated above.

One drawback of the XRD analysis is that it is a bulk technique compared to XRF, SEM/EDS, and it is not well suited to identify minor or trace phases in the aerosol samples. Therefore, it can be better utilized as a complementary technique with XRF and SEM/EDS.

ACKNOWLEDGEMENTS

The authors acknowledge the support of the Center for Advanced Materials Research Lab, University of Sharjah,

where the measurements were done. We also thank Dr. Hashem Stietiya, from Bee'ah, Sharjah for the useful discussions and hosting our sampling stations. N.M.H. acknowledges the support of the College of Arts and Sciences Dean's Office, at the American University of Sharjah.

- Achilleos, S., Wolfson, J. M., Ferguson, S. T., Kung, C. M., Hadjimitsis, D. G., Hadjicharalambous, M., Achilleos, C., Christodoulou, A., Nisanzi, A., Papoutsas, C., Themistocleous, K., Athanasatos, S., Perdikou, S., and Koutrakis, P. (2016). "Spatial variability of fine and coarse particle composition and sources in Cyprus," *Atmos. Res.* **169**, 255–270.
- Al Katheeri, E., Al Jallad, F., and Al Omar, M. (2012). "Assessment of gaseous and particulate pollutants in the ambient air in Al Mirfa City, United Arab Emirates," *J. Environ. Prot.* **3**(07), 640.
- Anderson, J. O., Thundiyil, J. G., and Stolbach, A. (2012). "Clearing the air: a review of the effects of particulate matter air pollution on human health," *J. Med. Toxicol.* **8**(2), 166–175.
- Bener, A., Dogan, M., Ehlayel, N., Shanks, N., and Sabbah, A. (2009). "The impact of air pollution on hospital admission for respiratory and cardiovascular diseases in an oil and gas-rich country," *Eur. Ann. Allergy Clin. Immunol.* **41**(3), 80.
- Gates-Rector, S. and Blanton, T. (2019). "The powder diffraction file: a quality materials characterization database," *Powd. Diffr.* **34**(4), 352–360.
- Hamdan, N. M., Alawadhi, H., and Jisrawi, N. (2015). "Elemental and chemical analysis of PM₁₀ and PM_{2.5} indoor and outdoor pollutants in the UAE," *Int. J. Environ. Sci. Dev.* **6**(8), 566.
- Hamdan, N. M., Alawadhi, H., and Jisrawi, N. (2016). "Particulate matter pollution in the United Arab Emirates: elemental analysis and phase identification of fine particulate pollutants." *Proceedings of the 2nd World Congress on New Technologies (NewTech'16)*, Budapest, Hungary, August 2016, pp. 18-19. International Academy of Science, Engineering and Technology (International ASET Inc.), Orléans, Ontario, Canada.
- Hamdan, N. M., Alawadhi, H., Jisrawi, N., and Shameer, M. (2018a). "Characterization of fine particulate matter in Sharjah, United Arab Emirates using complementary experimental techniques," *Sustainability* **10**(4), 1088.
- Hamdan, N. M., Alawadhi, H., Jisrawi, N., and Shameer, M. (2018b). "Size-resolved analysis of fine and ultrafine fractions of indoor particulate matter using energy dispersive X-ray fluorescence and electron microscopy," *X-Ray Spectrom.* **47**(1), 72–78.
- Ianniello, A., Spataro, F., Esposito, G., Allegrini, I., Hu, M., and Zhu, T. (2011). "Chemical characteristics of inorganic ammonium salts in PM_{2.5} in the atmosphere of Beijing (China)," *Atmos. Chem. Phys.* **11**(21), 10803–10822.
- Li, Y., Gibson, J. M., Jat, P., Puggioni, G., Hasan, M., West, J. J., Vizuete, W., Sexton, K., and Serre, M. (2010). "Burden of disease attributed to anthropogenic air pollution in the United Arab Emirates: estimates based on observed air quality data," *Sci. Total Environ.* **408**(23), 5784–5793.
- Moloi, K., Viksna, A., Selin, E., Lindgren, L., and Standzenieks, P. (2002). "Sequential leaching of trace elements in fine-particle aerosol samples on Teflon filters," *X-Ray Spectrom.* **31**(1), 27–34.
- National Centre for Meteorology and Seismology, United Arab Emirates (2019). "UAE climate yearly report 2003–2018." Available at <http://www.ncms.ae/en/climate-reportsyearly.html?id=26>
- Satsangi, P. and Yadav, S. (2014). "Characterization of PM_{2.5} by X-ray diffraction and scanning electron microscopy–energy dispersive spectrometer: its relation with different pollution sources," *Int. J. Environ. Sci. Technol.* **11**(1), 217–232.
- Song, X., Shao, L., Zheng, Q., and Yang, S., (2015). "Characterization of crystalline secondary particles and elemental composition in PM₁₀ of North China," *Environ. Earth Sci.* **74**(7), 5717–5727.
- Sundvor, I., Balaguer, N. C., Viana, M., Querol, X., Reche, C., Amato, F., and Guerreiro, C. (2013). "Road Traffic's Contribution to Air Quality in European Cities, ETC/ACM Technical Paper 2012/14." Copenhagen: European Topic Centre for Air Pollution and Climate Change Mitigation.
- Widziewicz, K., Rogula-Kozłowska, W., and Loska, K. (2016). "Cancer risk from arsenic and chromium species bound to PM_{2.5} and PM₁ – Polish case study," *Atmos. Pollut. Res.* **7**(5), 884–894.
- Wong, C. M., Tsang, H., Lai, H. K., Thomas, G. N., Lam, K. B., Chan, K. P., Zheng, Q., Ayres, J. G., Lee, S. Y., Lam, T. H., and Thach, T. H. (2016). "Cancer mortality risks from long-term exposure to ambient fine particle," *Cancer Epidemiol. Biomarkers Prev.* **25**(5), 839–845.
- Young, L. H., Liou, Y. J., Cheng, M. T., Lu, J. H., Yang, H. H., Tsai, Y. I., Wang, L. C., Chen, C. B., and Lai, J. S. (2012). "Effects of biodiesel, engine load and diesel particulate filter on nonvolatile particle number size distributions in heavy-duty diesel engine exhaust," *J. Hazard. Mater.* **199**, 282–289.